Pharmaceutical Research, Vol. 24, No. 6, June 2007 (© 2007)
DOI: 10.1007/s11095-007-9253-0

Research Paper

A Novel Method for Imaging *In Vivo* Degradation of Poly(L-Glutamic Acid), a Biodegradable Drug Carrier

Marites P. Melancon,[1] Wei Wang,[1] Yuetang Wang,[1] Ruping Shao,[1] Xiaojun Ji,[1] Juri G. Gelovani,[1] and Chun Li[1,2]

Received January 8, 2007; accepted January 26, 2007; published online March 22, 2007

Purpose. To develop an L-PG-based imaging probe suitable for assessing the degradation of L-PG *in vivo*.
Materials and Methods. Conjugates of L-PG and a near-infrared fluorescence (NIRF) dye, NIR813, were characterized with regard to quenching efficiency and degradability by cathepsin B (CB) and other proteases. The kinetics of L-PG-NIR813's degradation and its degradation in orthotopic human U87/TGL glioma in nude mice after intravenous injection was assessed using NIRF optical imaging ($n = 3$).
Results. The fluorescence signal from L-PG-NIR813 was efficiently quenched and activated at NIR813 loadings of 8–10%. Upon exposure to CB, the fluorescence intensity of L-PG-NIR813 increased 10-fold. L-PG-NIR813 was also degraded by another cysteine protease cathepsin L, but not by MMP-2, cathepsin E, cathepsin D, and plasmin. A selective CB inhibitor blocked the fluorescence activation. After intravenous injection, the degradation of L-PG-NIR813 was visualized primarily in the liver, which peaked at 4 h postinjection. Activation of L-PG-NIR813 but not D-PG-NIR813 was clearly seen in U87/TGL tumors.
Conclusion. Our results indicate that L-PG-NIR813 may be used to monitor the *in vivo* degradation of L-PG-based polymeric drugs, and that this agent may prove useful in noninvasive imaging of protease activity, particularly that of cysteine proteases.

KEY WORDS: biodegradation; cathepsin B; molecular imaging; near-infrared optical imaging; poly(L-glutamic acid).

INTRODUCTION

Poly(L-glutamic acid) (L-PG) has been used as a macromolecular carrier for drug delivery, specifically to target cancer (1). L-PG-paclitaxel (PG-TXL, CT2103, Xyotax) has advanced to phase III clinical trials, and L-PG-camptothecin (CT2106) has been tested in phase II clinical trials. Preclinical studies in a number of animal tumor models, including orthotopic and metastatic tumor models, demonstrated that PG-TXL exhibited significantly higher uptake in the tumors and greater antitumor activity than did the parent drug, paclitaxel (1).

A recent report confirmed that monoglutamyl-2′-TXL and diglutamyl-2′-TXL are the major intracellular metabolites of PG-TXL (2). Hydrolysis of these metabolites led to the release of free TXL. Specific enzyme inhibitors—such as CA-074 methyl ester, a cell-permeable irreversible inhibitor of cathepsin B (CB), and EST, a cell-permeable irreversible inhibitor of cysteine protease—decreased the formation of monoglutamate TXL and free TXL in a tumor cell line that had been incubated with PG-TXL (2). On the other hand, PG-TXL is relatively resistant to aqueous hydrolysis and plasma esterase. Less than 14% of bound TXL was released from PG-TXL incubated in buffered saline or plasma for 24 h at 37°C (3). These results suggest that selective proteolysis of the PG backbone through the action of cellular proteases in tumors may be responsible for the increased site-specific delivery and enhanced antitumor activity of L-PG-bound TXL.

The degradation of L-PG by lysosomal enzymes has been extensively studied *in vitro* using purified enzymes and cell lysates (4–7). These studies have shown that L-PG is more susceptible to lysosomal degradation than are poly(aspartic acid) and poly(D-glutamic acid) (D-PG) (8), and that cysteine proteases, particularly CB, play key roles in the lysosomal degradation of PG (4,6). However, studies of the kinetics of *in vivo* degradation of PG in various tissues in live animals have not been possible because of the lack of suitable technology. *In vivo* degradation of polymeric drugs can be studied by analyzing the appearance of degradation products in the target tissues. However, this method requires tissue biopsy, which cannot be performed repeatedly at the same site in the same species and often involves a tedious purification and analysis scheme. An imaging method that permits noninvasive assessment of the *in vivo* degradation of L-PG-drug conjugates would be useful in assessing the relationship between *in vivo* degradability and antitumor efficacy of L-PG-based therapeutic agents. Such a method may also guide L-PG-based therapeutics towards patients who may benefit the most from the therapy.

[1] Department of Experimental Diagnostic Imaging-Box 57, The University of Texas M. D. Anderson Cancer Center, 1515 Holcombe Boulevard, Houston, Texas 77030, USA.
[2] To whom correspondence should be addressed. (e-mail: cli@di.mdacc.tmc.edu)

In the current study, we synthesized and characterized a L-PG-based polymeric imaging probe consisting of L-PG and a near-infrared fluorescence (NIRF) dye. Fluorescently quenched L-PG became optically active upon polymer backbone degradation. The fluorescence signal thus generated was detected by NIRF optical imaging techniques.

MATERIALS AND METHODS

Materials

L-PG, D-PG, N-hydroxysuccinimde (NHS), N,N-diisopropylethylamine, IR-783 sodium acetate, ethylenediaminetetraacetic acid (EDTA), cysteine, phosphate-buffered saline (PBS), cathepsin D (an aspartic protease), cathepsin E (an aspartic protease), plasmin (a serine protease), cathepsin L (a cysteine protease), and CB (a cysteine protease) were purchased from Sigma-Aldrich (St. Louis, MO). Hydroxybenzotriazole (HOBt) and benzotriazol-1-yl-oxy-tris-pyrrolidino-phosphonium hexaflurophosphate (PyBOP) were purchased from Novabiochem (San Diego, CA). Trifluoroacetic acid (TFA) was obtained from Chem-Impex International, Inc. (Wood Dale, IL). 4-Mercaptobenzoic acid was purchased from TCI (Portland, Oregon). PD-10 columns were purchased from Amersham-Pharmacia Biotech (Piscataway, NJ). Spectra/Pro 7 dialysis tubing with molecular-weight cut-off of 10,000 was purchased from Fisher Scientific (Pittsburgh, PA). CB inhibitor II (Ac-Leu-Val-lysinal) and human recombinant matrix metalloproteinase-2 (MMP-2) (a metalloprotease) were purchased from Calbiochem (La Jolla, CA). All solvents were purchased from VWR (San Dimas, CA).

Analytical Methods

Gel permeation chromatography was performed on a Waters (Milford, MA) high-performance liquid chromatography (HPLC) system consisting of a 600 controller, a 717 plus auto sampler, and a Viscotek E-Z^{pro} triple detector (Viscotek, Houston, TX) that records refractive index, viscosity, and light-scattering signals. The samples were separated using a TSK-G4000PW 4.6 mm $\times$ 30 cm column (TosoHaas, Montgomeryville, PA) eluted with PBS containing 0.1% LiBr at a flow rate of 1.0 ml/min. Number-average molecular weights of the polymer conjugates were calculated using Viscotek TriSEC gel permeation chromatography software.

Analytical HPLC was carried out on an Agilent 1100 system (Wilmington, DE) equipped with a Vydac Peptide and Protein analytic C-18 column (Anaheim, CA). Sample was eluted with gradients of acetonitrile and H_2O containing 0.1% TFA.

Synthesis of NIRF Dye

NIRF dye containing a primary amine, IR-783-S-Ph-CONH$(CH_2)_5NH_2$, was synthesized in three steps. Briefly, IR-783-S-Ph-COOH was first synthesized from commercially available indocyanine dye IR-783 and 4-mercaptobenzoic acid according to the method of Strekowski *et al.* (9). IR-783-S-Ph-COOH was then conjugated to t-Boc-protected heterodiamine t-BocNH$(CH_2)_5NH_2$ using NHS activated ester. Finally, the resulting conjugate IR-783-S-Ph-CONH$(CH_2)_5$NHBoc was treated with 40% TFA in dichloromethane to give IR-783-S-Ph-CONH$(CH_2)_5NH_2$. Mass spectroscopy: M^+ 929.47 [calculated], 929.43 [found]. Yield: 86%. The fluorescence emission maximum for IR-783-S-Ph-CONH$(CH_2)_5NH_2$ was 813 nm. Consequently, this compound is termed NIR813 dye throughout the remainder of this paper.

Synthesis of L-PG-NIR813 and D-PG-NIR813

NIR813 was attached to the side chain carboxylic acid groups of PG (Fig. 1). Sodium salt of L-PG (number-average molecular weight, 17,500) or D-PG (number-average molecular weight, 17,500) was dissolved in H_2O and precipitated by acidification with 1 N HCl. The polymer precipitate was collected by centrifugation and lyophilized. The percentage of NIR813 dye used for each conjugate was calculated on the basis of the molar ratio of the dye and the repeating glutamic acid residue in PG polymers. PyBOP (2 eq) and HOBt (2 eq) were added to a solution of PG and NIR813 in dimethylformamide, and then N,N-diisopropylethylamine (4 eq) was added. The reaction mixture was stirred at room temperature for 2–4 h, until NIR813 was completely consumed as monitored by HPLC. The solvents were removed under vacuum. The residue was dissolved in PBS and purified using PD-10 columns eluted with PBS. The solution was dialyzed against H_2O overnight and lyophilized. The yields of polymer were around 60%. NIR813 loading in the polymeric conjugates was expressed as the percentage of repeating units to which NIR813 was attached.

Effect of NIR813 Loading on L-PG-NIR813 Quenching Efficiency and CB-mediated L-PG-NIR813 Activation

All fluorescence measurements were carried out at excitation wavelength of 765 nm using a Spex Fluorolog-3 spectrofluorimeter (Jobin Yvon Inc., Edison, NJ). Each L-PG-NIR813 solution (1 μM equivalent NR813) in water or NIR813 in methanol/water was placed in 1-cm quartz cuvette.

For the measurement of the effect of NIR813 loading on CB-mediated activation of L-PG-NIR813, CB (0.4 unit/ml)

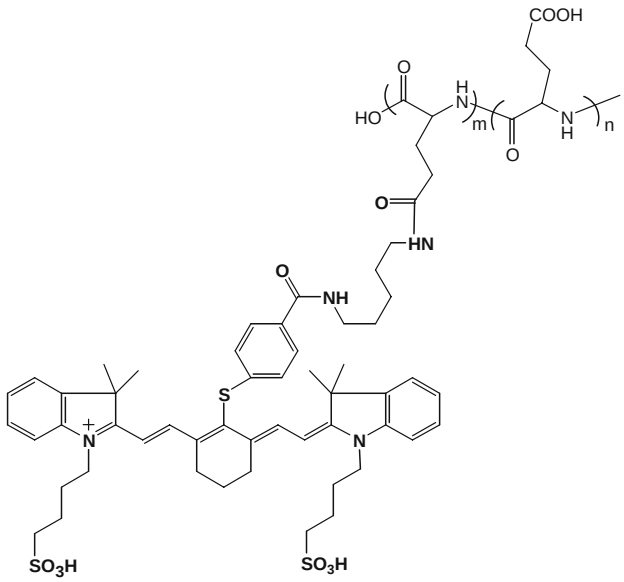

Fig. 1. Structures of PG-NIR813.

was added into the L-PG-NIR813 solution in the black microtiter wells. The plates were incubated at 37°C for 24 h and scanned at the 800-nm channel using an Odyssey Near-Infrared Imaging System (Lincoln, NE) for quantification of the fluorescence intensity. The data were expressed as percentage of recovered fluorescence intensity as a function of incubation time, calculated as $\text{Intensity}\% = \left(I_{t,\,\text{conjugate}} - I_{0,\,\text{conjugate}}\right)/\left(I_{0,\,\text{NIR813}} - I_{0,\,\text{conjugate}}\right)*100$, where $I_{t,\ \text{conjugate}}$ is the fluorescence intensity of polymeric conjugate at time t, $I_{0,\ \text{conjugate}}$ is the intensity of polymeric conjugate at time 0, and $I_{0,\ \text{NIR813}}$ is the intensity of free NIR813 at the same equivalent dye concentration. The percentage change in signal intensity for L-PG-NIR813 at 1% loading was presented as $\text{Intensity}\% = I_t/I_0*100$ because the intensity decreased rather than increased over time. The number-average molecular weight for both L-PG-NIR813 and D-PG-NIR813 was 17,500.

CB Activity Assays

CB activity was assayed with L-PG-NIR813 at pH 6.0. Various concentrations of L-PG-NIR813, from 0.625 to 25 μM, were incubated with 0.2 unit of CB at 25°C for 1 h. Fluorescence intensity was recorded every 3 min. The initial velocity (v) is the slope of the fluorescence intensity versus time curve calculated using the linear regression method. The Michaelis constant, K_m (substrate concentration at which the velocity of the enzyme-catalyzed reaction is half maximal), was determined by the Lineweaver-Burk method of plotting (10).

For studies of inhibitor kinetics, the activity of CB was adjusted to 0.2 units at pH 6.0. CB inhibitor II was preincubated with CB for 5 min, and then reactions were started by the addition of the substrate. The fluorescence of the degraded L-PG-NIR813 was monitored using an Odyssey Near-Infrared Imaging System as described above. The inhibition constant, K_i, was calculated by fitting plots of the reaction rate (ν) as a function of both the substrate concentration ([S]) and the inhibitor concentration ([I]) to the following equation (11):

$$\nu = \frac{V_{\max}}{\left(1 + \frac{K_m}{[S]}\right)\left(1 + \frac{[I]}{K_i}\right)} \quad (1)$$

Other Enzymatic Assays

To determine the specificity of PG-NIR813 degradation by proteases, PG-NIR813 (8% loading, 40 mM eq. NIR813) was incubated with cathepsin B (0.04 unit), cathepsin L (0.04 unit), cathepsin D (0.08 unit), cathepsin E (0.08 unit), plasmin (0.03 unit), or MMP-2 (50 ng) at 37 °C over a period of 24 h. The degradation of the polymer was assessed using the Odyssey Near-Infrared Imaging System set at the 800-nm channel. The buffer and pH value of the buffer used in the degradation studies were selected according to manufacturer provided procedures. The percent increase in fluorescence intensities were calculated as described previously.

Cell Culture and Tumor Models

Human glioma U87/TGL cells expressing luciferase were derived from U87 cells (American Type Cell Culture, Rockville, MD) (12). The U87 cell line was selected because of putative CB expression (13). Cells were maintained at 37°C in a humidified atmosphere containing 5% CO_2 in Dulbecco's modified Eagle's medium and nutrient mixture F-12 Ham (DMEM/F12) containing 10% fetal bovine serum (GIBCO, Grand Island, NY).

For the studies of *in vitro* degradation of PG-NIR813 by U87/TGL cells, cells were cultured in DMEM supplemented with 10% fetal bovine serum and antibiotics. When the cells grew to 85% confluence, they were trypsinized and seeded to 96-well black-wall plates (3×10^3 cells in 100 μl) at 37°C. Twenty-four hours later, PG-NIR813 (8.3%) at a final concentration of 5 μM eq. NIR813 was added. Degradation of PG-NIR813 was monitored at 0.2, 24, 48, and 72 h after the addition of the substrate. DMEM was used as a control.

Western Blot Analysis

For Western blot analysis, cell lysate was prepared using a mammalian cell lysis kit (Sigma, St. Louis, MO). Tumor specimens, extracted from U87/TGL tumors grown in mice (see below), were prepared by homogenization and then suspension in lysis buffer [20 mM Tris-HCl (pH 7.5), 150 nM NaCl, 0.1% sodium dodecyl sulfate, 1% Triton X-100, 1% sodium deoxycholate, 0.02 mM phenylmethylsulfonylfluoride, 0.1 nM NaF, 0.01 mM sodium orthovanandate, and 0.01 mg/ml aprotinin]). The protein concentration of the cell lysate and tumor homogenate was quantified using the Bradford method (14). One hundred micrograms of the proteins was used for Western blotting. Sodium dodecyl sulfate-polyacrylamide gel electrophoresis was performed with 10% gels, and proteins from the gel were electroblotted onto a nitrocellulose membrane (Bio-Rad, Hercules, CA). Immunodetection of CB and actin was accomplished by incubation with rabbit anti-CB antibody (1:500 diluted, Santa Cruz Biotechnology, Santa Cruz, CA) or mouse anti-actin monoclonal antibody (1:500, Sigma-Aldrich), followed by incubation with horseradish-conjugated anti-rabbit or anti-mouse antibody (1:5,000 diluted, Jackson ImmunoResearch laboratories Inc., West Grove, PA). Immunodetection was developed with SuperSignal West, followed by addition of Pico Chemiluminescent Substrate (Pierce Biotechnology, Rockford, IL).

In Vivo Imaging Study

All animal work was carried out in the Small Animal Imaging Facility at The University of Texas M. D. Anderson Cancer Center in accordance with institutional guidelines.

For imaging dynamics of polymer degradation, healthy female athymic nude mice (18–25 g; Harlan Sprague Dawley, Inc., Indianapolis, IN, $n = 3$) were injected intravenously with L-PG-NIR813 at a dose of 10 nmol eq. NIR813 per mouse. Whole-body optical imaging was done at various time points until 48 h using an IVIS imaging system (Xenogen Corp., Alameda, CA) equipped with indocyanine green filter sets (excitation/emission, 710–760/810–875 nm). The field of view was 13.1 cm in diameter. The fluency rate for NIRF excitation light was 2 mW/cm^2. The camera settings included maximum gain, 2×2 binning, 640×480 pixel resolution, and an exposure time of 0.8 sec. Prior to imaging, mice were

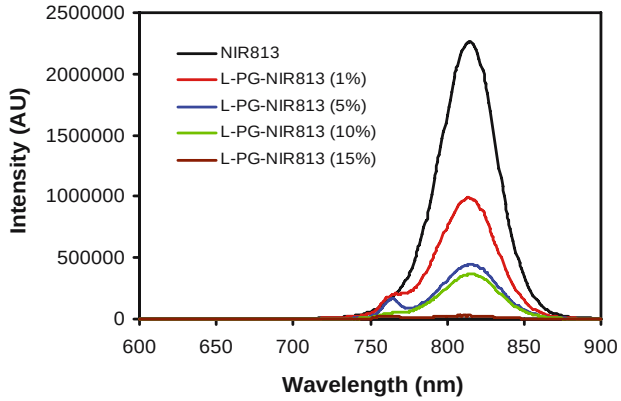

Fig. 2. Effect of NIR813 loading on the quenching efficiency of L-PG-NIR813. The number-average molecular weight of L-PG was 17,500. All conjugates had the same equivalent concentration of NIR813 (1 μM). Fluorescence intensity decreased with increasing payload of NIR813.

anesthetized with 2% isoflurane gas in oxygen. During imaging, mice were maintained in an anesthetized state with 0.5–1.5% isoflurane (Iso-Thesia, Rockville, NY) in oxygen.

Biodistribution study was performed in a separate experiment. Two groups of healthy nude mice consisting of three mice each were injected intravenously with L-PG-NIR813 or D-PG-NIR813, both at 10 nmol eq. NIR813. The mice were killed 4 h later. Major organs and blood were removed, imaged with a Xenogen camera, weighed, and their fluorescence intensities were calculated using LIVINGIMAGE v.2.11 software (Xenogen, Alameda, CA). Uptakes of contrast agent in various tissues were calculated as flux (photons/s) per gram of tissue. Student's *t* test was used to compare differences in tissue uptakes between the two agents, with *p* values less than 0.05 considered significant.

To compare degradation of L-PG-NIR813 and D-PG-NIR813 in U87/TGL tumors, athymic nude mice (National Cancer Institute, Bestheda, MD) were inoculated intracranially with U87/TGL cells. Briefly, aliquots of U87/TGL cell suspension (20 μL, 1.5×10^6 cells/mouse) were injected over a period of 3 min into the right parietal lobe of the brain using a Hamilton (Reno, NV) microtiter syringe connected to the manipulating stereotactic frame. The scalp wound was closed with Autoclips (Becton Dickinson, Sparks, MD). The animals were anesthetized with isoflurane as described above during surgery.

Tumor growth in the brains of the mice was monitored by using an IVIS imaging system to measure luciferase activity. Firefly D-luciferin (potassium salt, Xenogen Corp) was diluted to 0.5 mg/ml stock in PBS and was filtered through a 0.22-μm filter before use. Mice were anesthetized with isoflurane gas and were subsequently injected intravenously with D-luciferin at a dose of 5 mg/kg. Bioluminescence images were acquired 5 min after luciferin administration. The field of view was set at 13.1 cm in diameter. The camera settings included an exposure time of 10 s with 2×2 binning. After the bioluminescence imaging, mice bearing U87/TGL tumors with similar luminescence signal intensity were selected for NIRF imaging, which was performed as described previously. The gray-scale photographic images were superimposed with bioluminescent or NIRF color images using the LIVINGIMAGE v.2.11 software.

RESULTS

Characterization of PG-NIR813

To define the optimal loading of NIR813 dyes on L-PG for both efficient quenching and maintaining enzymatic degradability, L-PG-NIR813 conjugates of various NIR813 loadings were synthesized and their fluorescence spectra characterized (Fig. 2). At 1% NIR813 loading (1.2 dyes per polymer chain), signal intensity was reduced to 44% of that of NIR813. Increasing the NIR813 loading to 5% (six dyes per polymer chain) resulted in further reduction in signal intensity, to less than 20% of the signal intensity of the parent dye. Almost complete quenching (1% intensity remaining) was reached when the loading level of NIR813 on L-PG-NIR813 was 15% (Fig. 2).

The effects of NIR813 loading and the stereoisomeric structure of the PG polymer on CB-mediated fluorescence activation are presented in Fig. 3a. For L-PG-NIR813 contain-

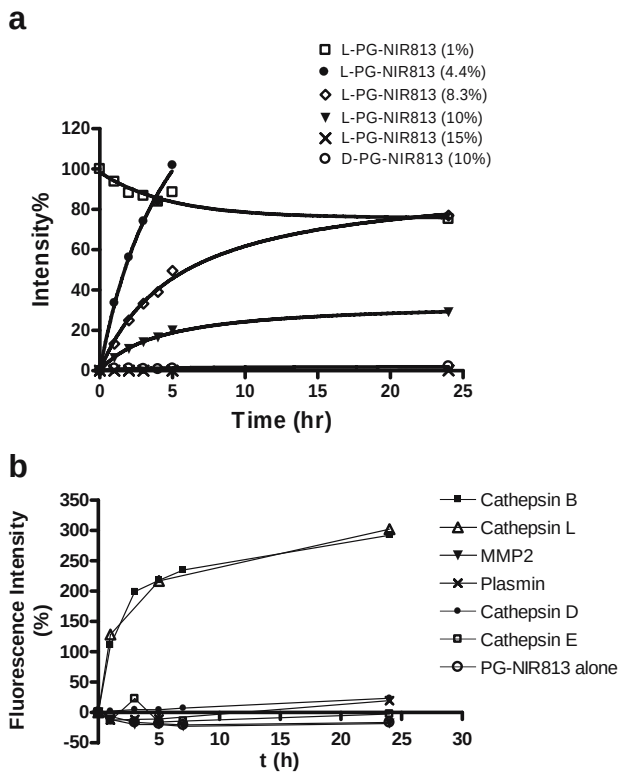

Fig. 3. **a**: Effect of NIR813 loading on degradation of L-PG-NIR813 in the presence of CB. Aliquots (100 μL) of each L-PG-NIR813 solution (10 μM equivalent NIR813) in 20 mM sodium acetate buffer (pH 5.2) were incubated with CB (0.4 units/ml) at 37°C for 24 h in triplicate. The data were acquired and analyzed as described in "Materials and Methods." The number-average molecular weight of both L-PG-NIR813 and D-PG-NIR813 was 17,500. **b**: Degradation of PG-NIR813 by proteases of different classes. PG-NIR813 (40 mM eq. NIR813) was incubated with CB (0.04 unit), cathepsin L (0.04 unit), cathepsin D (0.08 unit), cathepsin E (0.08 unit), plasmin (0.03 unit), or MMP-2 (50 ng) at 37-C over a period of 24 h. The buffer and pH value of the buffer used in the studies were selected according to manufacturer provided procedures. Fluorescence intensity only increased with the use of CB and cathepsin L. Data are presented as an average of duplicate experiments.

ing 4–10% NIR813, the percentage of recovered fluorescence intensity increased with increasing incubation time and plateaued by 24 h. At a lower loading (1%), there was a slight decrease in signal intensity over time, which may be attributed to the combined effect of lack of efficient quenching to begin with and gradual loss of fluorescence stability. At a higher loading (15%), the fluorescence signal remained quenched throughout the incubation period. For D-PG-NIR813 at a loading of 10%, no fluorescence signal was recovered over the 24-h incubation period (Fig. 3a). Because L-PG-NIR813 at a NIR813 loading of 8–10% exhibited excellent efficiency in terms of both fluorescence quenching and CB activation, these preparations were used in further studies. Figure 3b shows that fluorescence signal from L-PG-NIR813 was activated only upon exposure to cysteine proteases CB and cathepsin L, but not exposure to the other three classes of proteases.

Kinetics of L-PG-NIR813 Degradation by CB and Selectivity of Optical Activation

A double-reciprocal velocity versus substrate concentration plot for the enzymatic activity of CB on L-PG-NIR813 is shown in Fig. 4a. The K_m values derived for this reaction were 200 μM. K_m represents the dissociation constant (or affinity for substrate) of the enzyme-substrate complex. A relatively high K_m value for L-PG-NIR813 as compared to small molecular weight peptide substrates with Km values of 2–14 μM (15,16) indicates that PG-NIR813 and CB formed a loosely bound complex.

The degradation of L-PG-NIR813 by CB was inhibited by the selective CB inhibitor CB inhibitor II in a dose-dependent manner (Fig. 4b). To quantify the inhibitory activity of CB inhibitor II, the reaction rate as a function of the L-PG-NIR813 concentration at different concentrations of the inhibitor was determined. The data were fit to the standard equation for competitive inhibition (Eq. 1), yielding a K_i value of 69.5 ± 3.0 nM. This result and the linear double-reciprocal velocity versus substrate concentration plot suggested that CB inhibitor II was competitive against the L-PG-NIR813 substrate.

In Vitro Degradation of L-PG-NIR813 in U87/TGL Cells

Western blot analysis showed human CB expression in both U87/TGL cells and U87/TGL tumors (Fig. 5a). Incubation of L-PG-NIR813 in cultured U87/TGL cells resulted in significantly higher fluorescence signal intensity than that observed in culture medium during a period of 0.2–72 h (Fig. 5b).

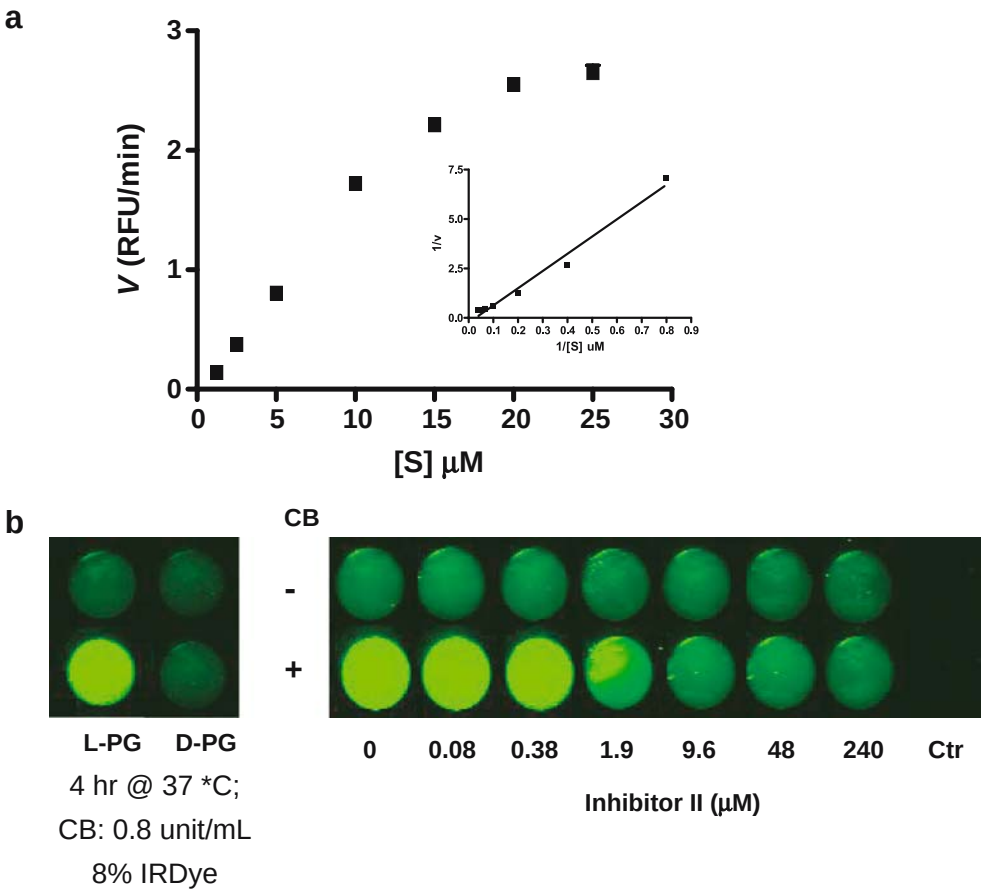

Fig. 4. Enzymatic degradation of L-PG-NIR813. **a:** Kinetics of polymer degradation by CB. Various concentrations of L-PG-NIR813, from 0.625 to 25 μM, were incubated with 0.2 units of CB at 25°C for 1 h, and the initial velocity value (v) was obtained as described in "Materials and Methods." The graph insets are Lineweaver-Burk plots of the transformed data. RFU, relative fluorescence units. **b:** Inhibition of L-PG-NIR813 degradation by CB inhibitor II. L-PG-NIR813 (8% loading; 10 μM eq. NIR813) was incubated with increasing concentrations of CB inhibitor II and 0.2 units of CB and imaged at 24 h as described in "Materials and Methods." No L-PG-NIR813 was added in control wells.

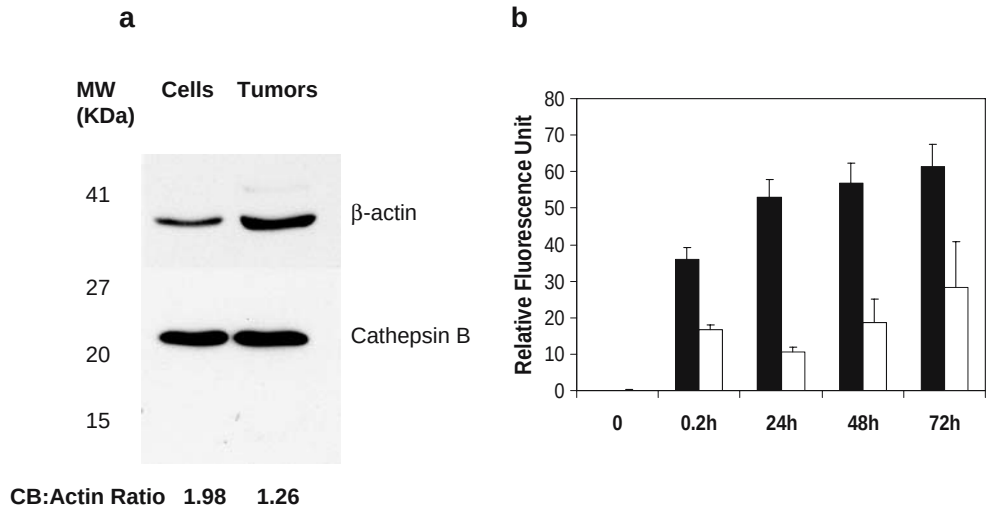

Fig. 5. Degradation of L-PG-NIR813 in U87/TGL cells. **a**: Western blot analysis of CB expression in U87/TGL cell lysate and excised U87/TGL tumors. **b**: *In vitro* degradation of L-PG-NIR813 in cultured U87/TGL cells as measured by activation of fluorescence signal. The data represent mean ± SD ($n = 3$). Note the significantly higher signal intensity from 0.2 to 72 h in U87/TGL cell culture (*closed square*) than in fresh culture medium (*open square*) ($p < 0.001$).

Imaging Results

Intravenous injection of L-PG-NIR813 into normal mice resulted in increased fluorescence intensity in the major organs. The fluorescence peaked at 4 h after injection and slowly declined over 48 h (Fig. 6a). At 4 h after intravenous injection, fluorescence activity in the lung, liver, kidney, intestine, and femur was significantly higher in mice injected with L-PG-NIR813 (molecular weight, 17,500) than in mice injected with D-PG-NIR813 (molecular weight, 17,500; $p < 0.05$) (Fig. 6b and c).

Ten days after inoculation, luciferase activity was clearly visualized in the brains of mice inoculated with U87/TGL cells. Mice with similar bioluminescence intensity (thus having similar tumor burden) were selected for imaging study (Fig. 7). At 4 h after injection of L-PG-NIR813 (molecular weight, 17,500) or D-PG-NIR813 (molecular

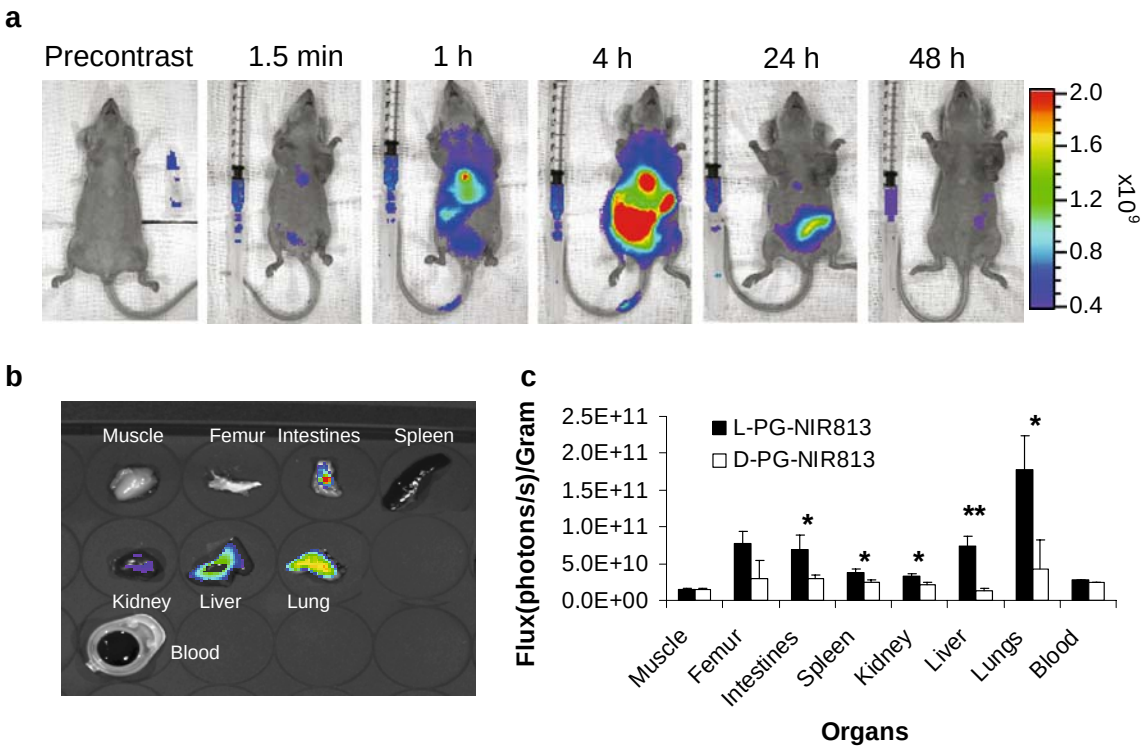

Fig. 6. *In vivo* degradation of L-PG-NIR813. **a**: Representative whole-body NIRF images acquired at the indicated times after intravenous injection of L-PG-NIR813 at a dose of 10 nmol eq. NIR813 per mouse. The activity seen in intact animals primarily arose from the liver and the gut. **b**: Representative NIRF images of excised tissues at 4 h after conjugate injection. **c**: Distribution of fluorescence signals in various tissues at 4 h after injection of L-PG-NIR813 or D-PG-NIR813. The data represent mean ± SD ($n = 3$) (*, $p < 0.05$; **, $p < 0.005$).

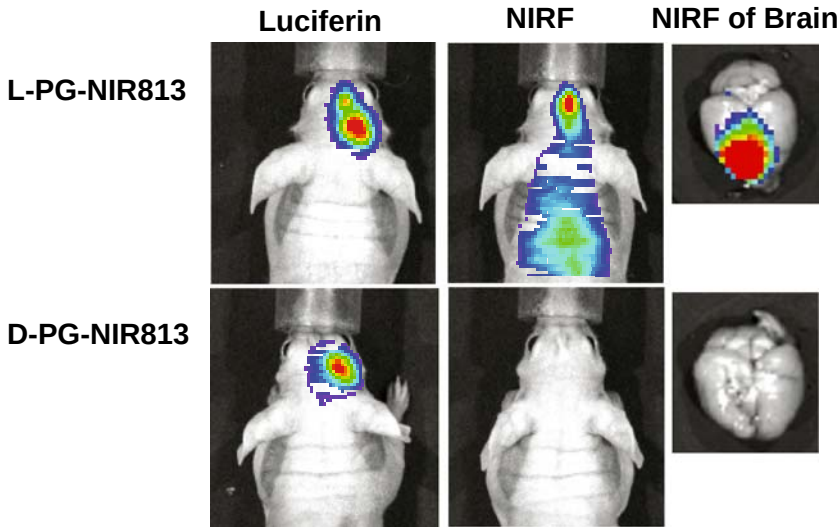

Fig. 7. Representative *in vivo* NIRF images of CB activity in intracranially inoculated U87/TGL tumors. The mice used in the study had the same tumor burden as indicated by bioluminescence signal generated after intravenous injection of luciferin. NIRF Images were acquired 24 h after intravenous injection of L-PG-NIR813 (50 nmol/mouse) or D-PG-NIR813 (50 nmol/mouse) with the same NIR dye loading (10%) and the same molecular weight (17,500). NIRF signal was visualized in the mouse injected with L-PG-NIR813 but not the mouse injected with D-PG-NIR813.

weight, 17,500), degradation of polymer and activation of fluorescence signal in the tumors were clearly visualized in mice injected with L-PG-NIR813 but not in mice injected with D-PG-NIR813. NIRF imaging of excised mouse brains confirmed the presence of fluorescence signal in the brains of mice injected with L-PG-NIR813 but not in the brains of mice injected with D-PG-NIR813 (Fig. 7), indicating degradation of L-PG-NIR813 but not D-PG-NIR813.

DISCUSSION

In this study, we synthesized and characterized a PG-based polymeric imaging probe suitable for assessing the *in vivo* degradation of L-PG-based polymer-drug conjugates. Recent studies have suggested that the antitumor activity of polymer-drug conjugates based on a biodegradable polymeric carrier, e.g., PG-TXL, may be directly related to the *in vivo* degradation of the polymer backbone and subsequent release of free drugs (2,17). Clinical data from phase III studies of PG-TXL in patients with non-small cell lung cancer (NSCLC) appear to support such a notion: among women with NSCLC who were premenopausal or had pretreatment estradiol levels >30 pg/ml, survival was better in patients who received PG-TXL than in those who received paclitaxel (18). It has been suggested that enhanced antitumor efficacy in patients with high estrogen levels may result from increased delivery of paclitaxel to lung cancer mediated through increased CB activity (17). A noninvasive imaging technique that allows repetitive assessment of the *in vivo* degradation of L-PG will facilitate studies of the relationship between various host factors and the degradation of the polymeric carrier at the tumor site.

Toward this end, we designed an imaging probe using an approach in which multiple NIRF dyes were attached to the side chain carboxyl groups of PG (Fig. 1). In this design, the conjugate is optically silent in its native (quenched) state and becomes highly fluorescent after degradation of the polymer backbone. The use of a dye that emits fluorescent light in the near-infrared region (650–900 nm) is necessary because hemoglobin and water, which are the major absorbers of visible and infrared light, respectively, have their lowest absorption coefficient in this region (19,20). A similar approach using polyethylene glycol-grafted poly(L-lysine) as a polymeric carrier and Cy5.5 as a NIRF dye has previously been used for imaging CB activity (21).

The loading of dye in L-PG-NIR813 is critical for optimal performance. At lower loading (<1%), only limited quenching was observed, while at higher loading (>15%), the imaging probe could not be activated, presumably because increased steric hindrance prevented the enzymes from approaching the substrate (Figs. 2 and 3).

Several of our observations, taken together, suggest that L-PG-NIR813 was degraded selectively by cysteine proteases. First, the degradation of L-PG-NIR813 by CB was inhibited by a specific CB inhibitor in a dose-dependent manner (Fig. 4b). Second, exposure of PG-NIR813 to several other proteases, including matrix metalloproteinase 2, cathepsin D, cathepsin E, and plasmin, did not produce measurable fluorescence signal resulting from probe activation (Fig. 3b), suggesting that these enzymes were not active in promoting the degradation of L-PG-NIR813. Because elevated levels of CB and cathepsin L have been found to correlate with invasive and metastatic profiles in both experimental cancer models and human malignancies (22,23), L-PG-NIR813 may be used as a probe for sensing *in vivo* cysteine protease activity.

The degradation of L-PG-NIR813 was clearly visualized at 1 h after injection, and the fluorescence intensity peaked by 4 h after injection (Fig. 6a). Significantly higher fluorescence activity was observed in the lung, liver, kidney, intestine, and femur of mice injected with L-PG-NIR813 than in those injected with D-PG-NIR813 (Fig. 6c). L-PG-NIR813 degradation products were cleared from the body primarily through the hepatobiliary system. It is possible that the fluorescence signal observed in different organs may be due to redistribution of degraded products. However, our previous studies with indium-111-labeled oligomeric glutamic acid showed that after intravenous injection, low-molecular-weight

species were rapidly cleared from the body through the renal system without retention in major organs, including liver and lung (24). Moreover, L-PG-NIR813 was not degradable in the presence of plasmin, a major blood protease (Fig. 3b). Therefore, it is unlikely that redistribution of degradation products would account for the enhanced fluorescence signal in such organs as femur and lungs in mice injected with L-PG-NIR813. Further work is needed to investigate the implications of degradation and retention of L-PG-NIR813 in the lungs in light of the recent clinical findings of antitumor activity of PG-TXL in women with lung cancer (18).

To evaluate whether the degradation of L-PG-NIR813 in tumors could be imaged in live animals, we used an orthotopic human glioma U87/TGL model. The expression of CB in both U87/TGL cells and tumors and the degradation of L-PG-NIR813 in cultured U87/TGL cells were first confirmed *in vitro* (Fig. 5). NIRF imaging study revealed that in U87/TGL tumors, fluorescence activation occurred only with L-PG-NIR813 but not with D-PG-NIR813 (Fig. 7), indicating that the observed fluorescence signal resulted from polymer backbone degradation rather than from the release of the dye from its side chains.

Limitation of the present work includes the lack of direct proof for enzymes responsible for the *in vitro* and *in vivo* degradation of L-PG-NIR dye in the U87 tumors, although the involvement of CB and cathepsin L were implicated. More specific CB inhibitors could be used to study the inhibition of polymer degradation in complex biological matrix. These issues are the subject of our ongoing investigations.

In conclusion, we have developed an optical imaging probe suitable for monitoring *in vivo* degradation of L-PG-based polymer-drug conjugates. This probe may also be used to assess enzymatic activity of cysteine proteases particularly that of CB and cathepsin L, in whole animals and in tumors. Since the enzymatic degradability of L-PG-drug conjugates is influenced by the physicochemical properties of the drug molecules attached to L-PG (4–7), caution should be taken when attempts are made to apply what we learned with L-PG-NIR813 to other L-PG drug conjugates, e.g., to PG-TXL. Nevertheless, L-PG-NIR813 will be a useful tool for studying the effect of various host factors on the degradation of L-PG polymer. The results of such studies may further our understanding of the antitumor activity of PG-TXL and other L-PG-based therapeutic agents.

ACKNOWLEDGMENTS

We would like to thank the National Institutes of Health (grants R01 CA119387 and R01 EB003132) and the John S. Dunn Foundation for financial support of this work.

REFERENCES

1. C. Li. Poly (L-glutamic acid)—anticancer drug conjugates. *Adv. Drug Deliv. Rev.* **54**:695–713 (2002).
2. J. W. Singer, S. Shaffer, B. Baker, A. Bernareggi, S. Stromatt, D. Nienstedt, and M. Besman. Paclitaxel poliglumex (XYOTAX; CT-2103): an intracellularly targeted taxane. *Anticancer Drugs.* **16**:243–254 (2005).
3. C. Li, R. A. Newman, Q. P. Wu, S. Ke, W. Chen, T. Hutto, Z. Kan, M. D. Brannan, C. Charnsangavej, and S. Wallace. Biodistribution of paclitaxel and poly(L-glutamic acid)-paclitaxel conjugate in mice with ovarian OCa-1 tumor. *Cancer Chemother. Pharmacol.* **46**:416–422 (2000).
4. H. C. Chiu, P. Kopeckova, S. S. Deshmane, and J. Kopecek. Lysosomal degradability of poly(alpha-amino acids). *J. Biomed. Mater. Res.* **34**:381–392 (1997).
5. C. J. T. Hoes, W. Potman, W. A. R. Van Heeswijk, J. Mud, B. G. de Grooth, J. Greve, and J. Feijen. Optimization of macromolecular prodrugs of the antitumor antibiotic Adriamycin. *J. Control. Release.* **2**:205–213 (1985).
6. L. A. McCormick-Thomsonand and R. Duncan. Poly (amino acid) copolymers as a potential soluble drug delivery system. 1. Pinocytic uptake and lysosomal degradation measured *in vitro*. *J. Bioact. Compat. Polym.* **4**:242–251 (1989).
7. W. G. Miller. Degradation of synthetic polypeptides. II. degradation of poly-L-glutamic acid by proteolytic enzymes in 0.20 M sodium chloride. *J. Am. Chem. Soc.* **86**:3913–3918 (1964).
8. B. K. Kishore, P. Lambricht, G. Laurent, P. Maldague, R. Wagner, and P. M. Tulkens. Mechanism of protection afforded by polyaspartic acid against gentamicin-induced phospholipidosis. II. Comparative *in vitro* and *in vivo* studies with poly-L-aspartic, poly-L-glutamic and poly-D-glutamic acids. *J. Pharmacol. Exp. Ther.* **255**:875–885 (1990).
9. L. Strekowski, T. Gorecki, J. C. Mason, H. Lee, and G. Patonay. New heptamethine cyanine reagents for labeling of biomolecules with a near-infrared. *Chromophore. Heterocycl. Commun.* **7**:2117–2122 (2001).
10. H. Lineweaver and D. Burk. *J. Amer. Chem. Soc.* **58**:658, 1934 (1934).
11. R. Copeland. Enzymes: A practical introduction to structure, mechanism, and data analysis. Wiley-VCH, 2000, p. 267–269.
12. V. Ponomarev, M. Doubrovin, I. Serganova, J. Vider, A. Shavrin, T. Beresten, A. Ivanova, L. Ageyeva, V. Tourkova, J. Balatoni, W. Bornmann, R. Blasberg, and J. Gelovani Tjuvajev. A novel triple-modality reporter gene for whole-body fluorescent, bioluminescent, and nuclear noninvasive imaging. *Eur. J. Nucl. Med. Mol. Imaging.* **31**:740–751 (2004).
13. K. I. Hulkower, C. C. Butler, B. E. Linebaugh, J. L. Klaus, D. Keppler, V. L. Giranda, and B. F. Sloane. Fluorescent microplate assay for cancer cell-associated cathepsin B. *Eur. J. Biochem.* **267**:4165–4170 (2000).
14. M. M. Bradford. A rapid and sensitive method for the quantitation of microgram quantities of protein utilizing the principle of protein-dye binding. *Anal. Biochem.* **72**:248–254 (1976).
15. K. Stachowiak, M. Tokmina, A. Karpinska, R. Sosnowska, and W. Wiczk. Fluorogenic peptide substrates for carboxydipeptidase activity of cathepsin B.. *Acta. Biochim. Pol.* **51**:81–92 (2004).
16. M. Szabelski, M. Rogiewicz, and W. Wiczk. Fluorogenic peptide substrates containing benzoxazol-5-yl-alanine derivatives for kinetic assay of cysteine proteases. *Anal. Biochem.* **342**:20–27 (2005).
17. C. Allievi, I. Strepponi, U. Bastrup, L. Piazzoni, S. Tavazzi, R. Pisano, G. Pezzoni, M. Fornasier, A. Bernareggi, and J. W. Singer. Biodistribution of paclitaxel poliglumex (PPX) in lung: analysis of gender-related alterations in a preclinical model. *J. Clin. Oncol.* **24**:Abstract #17003 (2006).
18. H. Ross, P. Bonomi, C. Langer, M. O'Brien, K. O'Byrne, L. Paz-Ares, A. Sandler, M. Socinski, F. Oldham, and J. Singer. Effect of gender on outcome in two randomized phase III trials of paclitaxel poliglumex (PPX) in chemo-naïve pts with advanced NSCLC and poor performance status (PS2). *J. Clin. Oncol.* **24**:Abstract # 7039 (2006).
19. R. Weissleder and V. Ntziachristos. Shedding light onto live molecular targets. *Nat. Med.* **9**:123–128 (2003).
20. M. Gurfinkel, S. Ke, X. Wen, C. Li, and E. M. Sevick-Muraca. Near-infrared fluorescence optical imaging and tomography. *Dis. Markers.* **19**:107–121 (2003).
21. R. Weissleder, C. H. Tung, U. Mahmood, and A. Bogdanov Jr. *In vivo* imaging of tumors with protease-activated near-infrared fluorescent probes. *Nat. Biotechnol.* **17**:375–378 (1999).
22. T. Nomura and N. Katunuma. Involvement of cathepsins in the invasion, metastasis and proliferation of cancer cells. *J. Med. Invest.* **52**:1–9 (2005).
23. S. Roshy, B. F. Sloane, and K. Moin. Pericellular cathepsin B and malignant progression. *Cancer Metastasis. Rev.* **22**:271–286 (2003).
24. X.-Y. Cao, S. Ke, Q.-P. Wu, J. Gelovani, and C. Li. Optical and nuclear imaging of bone with poly (L-glutamic acid). *Molecular Imaging.* **3**:275, 2004 (2004).